Section 8

Development of and advances in ocean modelling and data assimilation, sea-ice modelling, wave modeling

Forecasting Wind-Waves at the North American Great Lakes

Jose-Henrique Alves[1,2], Arun Chawla[2]

1 Systems Research Group Inc
2 Environmental Modelling Center, NOAA/NCEP, US National Weather Service
Henrique.Alves@noaa.gov

The US National Weather Service (NWS) provides operational forecasts of wind-waves to the North American Great Lakes since 2004. In its initial implementation, the GLW ran on a regular spherical grid with approximately 4km spatial resolution. Recent upgrades to the GLW have increased the spatial resolution to 2.5km, also making it the first operational wave forecasting system in a major international operational center to use a curvilinear grid. The latter has allowed NCEP to generate wave forecasts on a Lambert conformal grid, addressing the needs of NWS forecasters and increasing the computational efficiency of the underlying WAVEWATCH III® model (Tolman et al., 2002). Details of the curvilinear grid implementation used in the GLW are provided in Rogers & Campbell (2009). Figure 1 illustrates the curvilinear GLW grid.

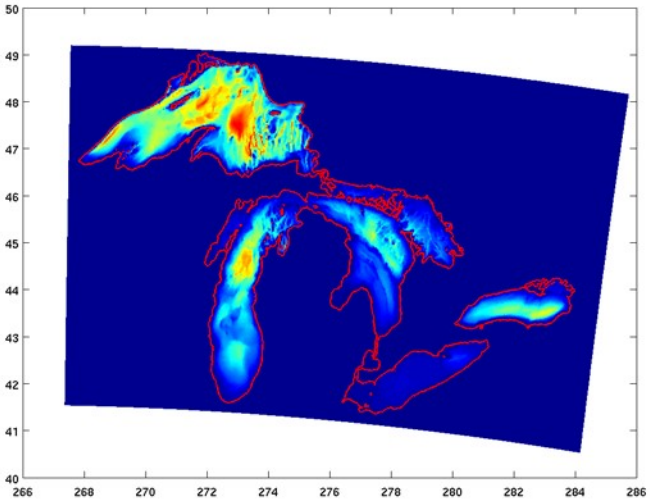

Figure 1 Curvilinear grid used in NCEP's Great Lakes wave forecast system (GLW).

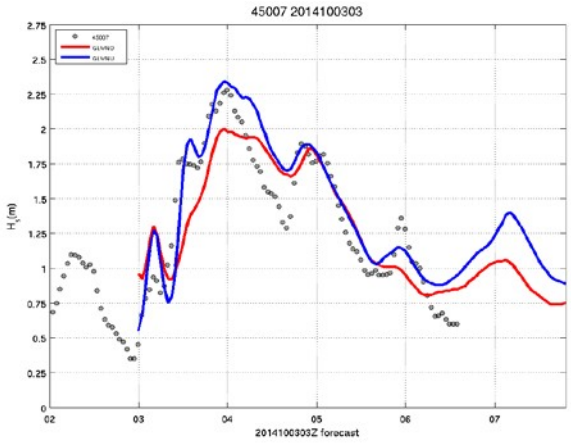

Figure 2: Significant Wave Height (Hs) at buoy 45007 (Lake Michigan).X-axis: Days of the month in Oct 2013.

Figure 2 shows the impact of the spatial resolution increase to GLW forecasts at a buoy maintained by the National Data Buoy Center (NDBC/NOAA), in Lake Michigan, made during a severe sea-state event on 03 Oct 2013. Circles indicate measurements of significant wave height in meters. The red line shows the performance of the model using a 4 km grid, whereas the blue line illustrates model results from the upgraded, 2.5 km curvilinear grid. In both cases, the same wind input was used, from NCEP's regional NAM model. The improvement is striking not only in terms of the skill in predicting the highest waves, but also in better defining the observed variations in wave height during the event.

In addition to changes in the spatial grid, recent upgrades to the GLW system included changing the source-term packages from the original WAVEWATCH III default configuration, consisting of wave-growth parameterizations proposed by Tolman & Chalikov (1996), to the newer source term package proposed by Ardhuin et al. (2010). The new source-term package has allowed the GLW to

dramatically improve its skill in predicting rapid wave growth in storms that develop under the more constrained Great Lakes environments. The new package also resulted in improved performance under normal sea-states and the typical wave generation conditions found in the region.

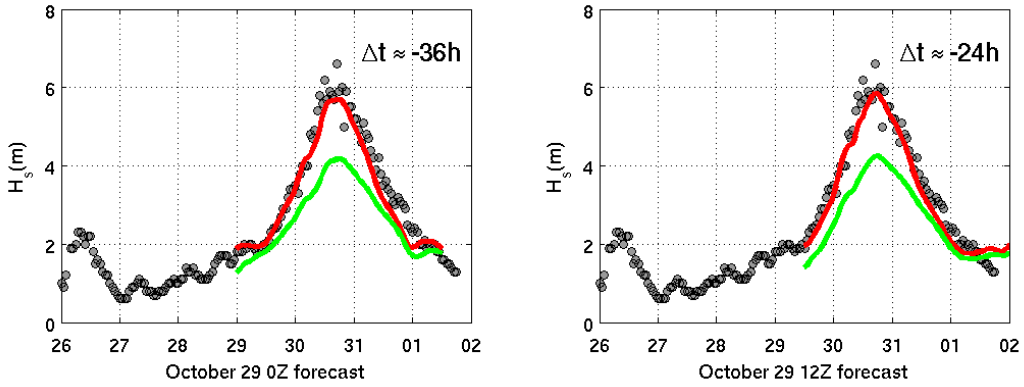

Figure 3 GLW wave forecasting system forecasts during the passage of post-tropical storm Sandy (Oct 2012)

Figure 3 illustrates the impact of the new source term parameterizations to wave forecasts issued by the GLW system during the passage of post-tropical storm Sandy (Oct 2012) over the Great Lakes. Circles indicate measurements of significant wave height in meters made at the NDBC buoy 45007 (Lake Michigan). The green line shows the performance of the model using the Tolman & Chalikov (1996) source-term package, whereas the red line illustrates model results from the upgraded package of Ardhuin et al. (2010). The improvements are striking for both 36 h and 24 h forecasts of maximum waves observed during Sandy. A detailed description of the GLW system and the impacts of upgrading its source-terms is provided in Alves et al. (2014).

In association with increased spatial resolution grids, source-term changes made in the GLW system have significantly improved the quality of forecasts issued by NCEP to NWS and the general public. As a consequence, the GLW system has become the major source of wave guidance used by NWS forecasters in the Great Lakes region.

References

Alves, J. H. G., Chawla, A., Tolman, H. L., Schwab, D., Lang, G., & Mann, G. (2014). The Operational Implementation of a Great Lakes Wave Forecasting System at NOAA/NCEP*. *Weather and Forecasting*, 29(6), 1473-1497.

Ardhuin, F., Rogers, E., Babanin, A., Filipot, J.-F., Magne, R., Roland, A., van der Westhuysen, A., Queffeulou, P., Lefevre, J.-M., Aouf, L., and Collard, F. (2010). Semi-empirical dissipation source functions for wind-wave models: part I, definition, calibration and validation. *J. Phys. Oceanogr.*, 40(9):1917–1941.

Rogers, W. E., and T. J. Campbell, 2009. Implementation of Curvilinear Coordinate System in the WAVEWATCHIII Model. *NRL Memorandum Report*: NRL/MR/7320-09-9193, 42 pp.

Tolman, H., and Chalikov, D.. Source terms in a third-generation wind wave model. *Journal of Physical Oceanography* 26.11 (1996): 2497-2518.

Tolman, H. L., Balasubramaniyan, B., Burroughs, L. D., Chalikov, D. V., Chao, Y. Y., Chen, H. S., & Gerald, V. M. (2002). Development and implementation of wind-generated ocean surface wave models at NCEP. *Weather and Forecasting*, 17(2), 311-333.

Probabilistic Wave Forecasting and Ensemble-Based Data Assimilation at the US National Weather Service

Jose-Henrique Alves[1,2], Natacha Bernier[3], Arun Chawla[2], Paula Etala[4], Paul Wittmann[5]

[1]Systems Research Group Inc
[2]Environmental Modelling Center, NOAA/NCEP, US National Weather Service
[3]Canadian Meteorological Center, Environment Canada
[4]Naval Hydrographic Service, Argentina
[5]Fleet Numerical Meteorology and Oceanography Center, US Navy
Henrique.Alves@noaa.gov

The National Centers for Environmental Prediction (NCEP) global wave ensemble system (GWES) has been providing operational wave forecasts for the US National Weather Service (NWS) since 2008. The GWES consists of a 20-member ensemble forced with NCEP-GEFS bias-corrected wind data, and one control run with NCEP's deterministic GFS model. After upgrades undertaken in July 2014, the GWES runs on a spherical grid with 1/2° resolution in longitude and latitude, and uses an efficient wave-generation physics package following Ardhuin et al. (2010). The current system provides high-quality deep-water wave forecasts, also generating products for applications in nearshore areas and under hurricane forcing conditions, a feature that results from a close interaction between three NCEP centers: the Environmental Modeling Center (EMC), the National Hurricane Center (NHC), and the Ocean Prediction Center (OPC). An example of output from the GWES[1] is provided in Figure 1.

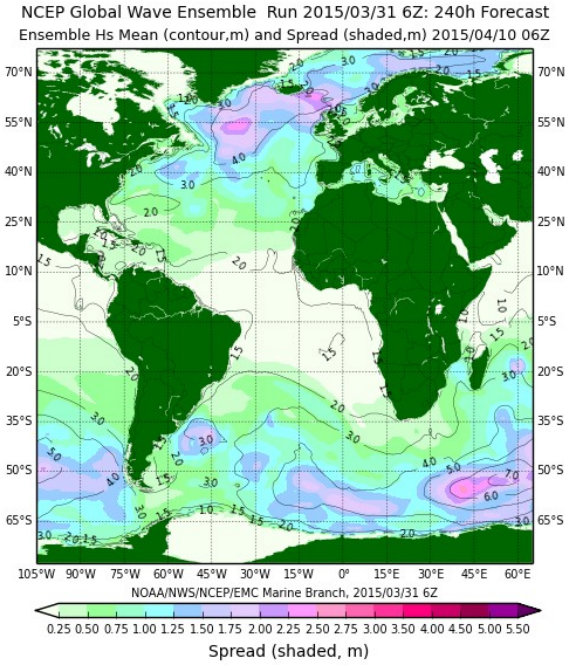

Figure 1 Graphical output from the GWES for 31 Mar 2015

Since 2011, the NWS and the US Navy have combined outputs from their global wave ensemble systems into the first operational multi-center forecast system providing probabilistic ocean wave forecasts. Products from the NCEP/FNMOC Combined Wave Ensemble (NFCENS) are distributed by the NWS and made available to the general public. Computed from 41 combined wave ensemble members, the new product outperforms deterministic and probabilistic forecasts and nowcasts of significant wave heights (Hs) issued separately at each forecast center, at all forecast ranges. Detailed results are described in Alves et al. (2013).

[1] GWES forecasts are made available via ftp://ftp.ncep.noaa.gov/pub/data/nccf/com/wave/prod/ and http://polar.ncep.noaa.gov/waves/viewer.shtml.

The successful implementation of the NFCENS has brought new opportunities for collaboration with Environment Canada (EC). EC is in the process of adding new global wave model ensemble products to its existing suite of operational regional products. The planned upgrade to the current NFCENS wave multi-center ensemble includes the addition of 20 members from the Canadian WES. With this upgrade, the NFCENS will be renamed the North American Wave Ensemble System (NAWES). As part of the new system implementation, new higher-resolution grids and upgrades to model physics using recent advances in source-term parameterizations are being tested.

Through a collaboration with the Argentinian Naval Hydrographic Service, NCEP is developing an ensemble-based data assimilation system, consisting of an implementation into the GWES of the 4D-LETKF proposed by Etala et al. (2015). The 4-D scheme initializes a full 81-member ensemble in a 6-hour cycle. The LETKF determines the analysis ensemble locally in the space spanned by the ensemble, as a linear combination of the background perturbations. Observations from three altimeters and one scatterometer are used. Preliminary results from a prototype system running at NCEP are shown in Figure 2. Note that the LETKF allows for introducing innovations to the analysed wave heights over a wider region than other conventional data assimilation approaches, which is a welcome feature considering the usually sparse wave data available globally.

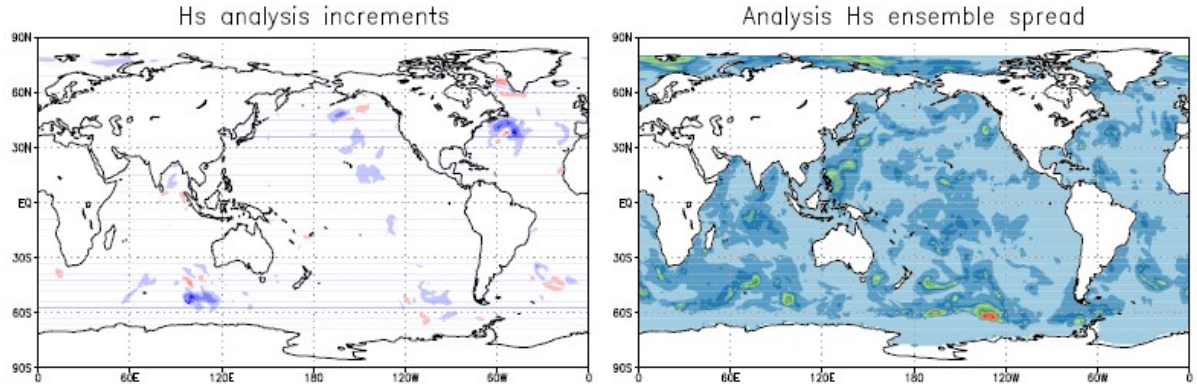

Figure 2 LETKF analysis increments for the ensemble mean significant wave height, 18 Sep 2014 00UTC.

References

Alves, Jose-Henrique GM, et al. "The NCEP-FNMOC Combined Wave Ensemble Product: Expanding Benefits of Interagency Probabilistic Forecasts to the Oceanic Environment." *Bulletin of the American Meteorological Society* 94.12 (2013): 1893-1905.

Ardhuin, F., Rogers, E., Babanin, A., Filipot, J.-F., Magne, R., Roland, A., van der Westhuysen, A., Queffeulou, P., Lefevre, J.-M., Aouf, L., and Collard, F. (2010). Semi-empirical dissipation source functions for wind-wave models: part I, definition, calibration and validation*. J. Phys. Oceanogr.*, 40(9):1917–1941.

Etala, Paula, Martín Saraceno, and Pablo Echevarría. "An investigation of ensemble-based assimilation of satellite altimetry and tide gauge data in storm surge prediction." *Ocean Dynamics* 65.3 (2015): 435-447.

Impact of physics upgrades to NCEP's wave modeling suites

Arun Chawla[1], Jose-Henrique Alves[2], Yung Chao[1], Vera Gerald[1], Deanna Spindler[3]

[1] Marine Modeling & Analysis Branch, EMC, NCEP, NWS

[2] SRG at Marine Modeling & Analysis Branch, EMC, NCEP, NWS

[3] IMSG at Marine Modeling & Analysis Branch, EMC, NCEP, NWS

arun.chawla@noaa.gov

Introduction

The Environmental Modeling Center (EMC) of the National Centers for Environmental Prediction (NCEP) is tasked with providing numerical guidance for forecasts of wind driven short waves for the National Weather Service (NWS). EMC maintains a range of wave modeling suites[1] – the global ocean wave, the hurricane wave, the ensemble wave and the regional Great Lakes wave modeling suites. All of these models are driven by the multi-grid WAVEWATCH III® driver (Tolman, 2008), using the default physics package of Tolman and Chalikov (1996). In the summer of 2012 EMC started upgrading the physics package in its modeling suites. This upgrade is now complete and this document reflects the increase in model skill in the global and hurricane wave systems. The Great Lakes and Ensemble wave modeling systems are reported on in separate documents.

Physics Package

The new physics package that has been implemented in the NCEP operational models is the Ardhuin et al. (2010) physics package. This package uses a wind input term that follows the ECWAM input (Janssen, 2004) very closely, with some reduction for high frequency and high wind input. The dissipation formulation includes a swell dissipation term and a wave breaking term that is made up of a saturation based dissipation term and a cumulative wave breaking term.

Results

A multi-grid modeling system has been in operations at NCEP since the beginning of 2008. This multi-grid system consists of a mosaic of two way nested grids with resolutions ranging from 0.5° – 0.067°. The new physics package was introduced into the global wave model in May 2012. Figure 1 shows the model skill scores since 2008. The skill scores have been computed using month long records

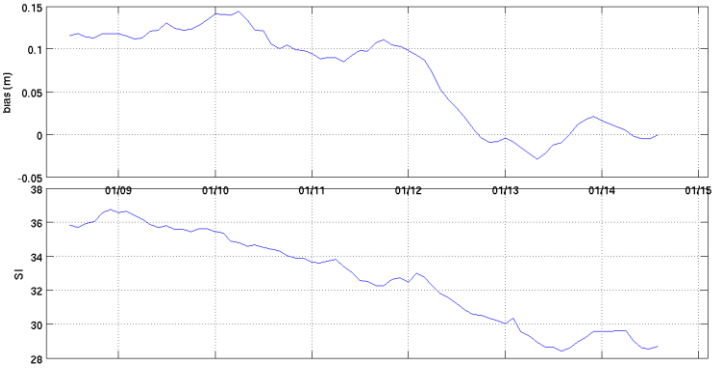

Figure 1: Skill scores of the global wave model for the 72 hour forecast. The x axis represents time as MM/YY.

[1] A new modeling system that is being developed for the near shore region is described in a separate paper

from all the available buoys maintained by the National Data Buoy Center (NDBC). A running average is used to remove seasonal patterns. Skill scores include the model bias and Scatter Index. Overall there has been a regular improvement in model skill due to improvements in wind guidance. However, a big limitation of the earlier physics package in the wave model was the inadequate dissipation of the swell fields, particularly of swells traveling across the Pacific Ocean. The new physics package takes care of this issue as can be clearly seen in the overall reduction in model bias beginning in early 2012. A spatial plot of model biases (figure not shown here) clearly shows this trend.

The new physics package was also introduced into the hurricane wave system, which is driven by a combination of global winds (outside the hurricane domain) and hurricane model winds (inside the hurricane domain). The hurricane domains cover the Western Atlantic (US East Coast) and Eastern Pacific (US West Coast) waters. Figure 2 shows the comparison of the overall wave energy (represented by the significant wave height here) at NDBC buoy 41001 as hurricane Sandy went past the buoy. The overall build up in wave energy is well represented in both physics packages, but the response of the new physics is much better as the eye of the hurricane (indicated by the drop and subsequent increase in wave height) passes near the buoy. This was true at other buoy locations as well as for other hurricanes. Apart from overall wave energy, the new physics package has a much better representation of the wave spectra in the model (figure not shown) leading to a better prediction of swell arrival times.

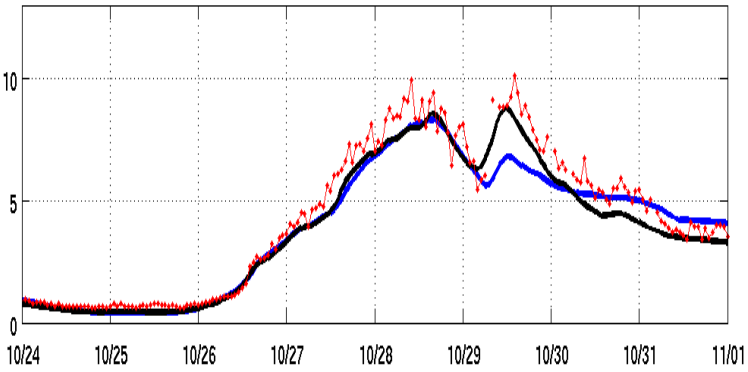

Figure 2: Significant wave height (Hs) at NDBC buoy 41001 during hurricane Sandy. Red - data ; Blue - old physics ; Black - new physics. X axis is time in MM/DD format

In conclusion, the new physics package does a better job in representing the processes associated with wave dynamics across multiple scales and has improved skill scores in all model system suites in operation at NCEP.

References

Ardhuin, F., W. E. Rogers, A. V. Babanin, J. Filipot, R. Magne, A. Roland, A. van der Westhuysen, P. Queffeulou, J. Lefevre, L. Aouf and F. Collard, 2010 : Semiempirical dissipation source functions for ocean waves. Part I: Definition, calibration and validation, *J. Phys. Oceanogr.*, **40**, 1,917 – 1,941

Janssen, P. A. E. M., 2004 : The interaction of ocean waves and wind. *Cambridge University Press.*

Tolman, H. L. and D. V, Chalikov, 1996 : Source terms in a third generation wind wave model, *J. Phys. Oceanogr.*, **26**, 2,497 – 2,518

Tolman, H. L., 2008 : A mosaic approach to wind wave modeling. *Ocean Mod.,* **25,** 35 – 47

Using Neural Network Technique to Enhance Assimilating Surface Satellite Observation into Numerical Models.

Vladimir Krasnopolsky[1], Carlos J. Lozano[1], Hae-Cheol Kim[2], Bin Li[2]
[1]NWS/NCEP/EMC, [2]IMSG at NWS/NCEP/EMC
Email: vladimir.Krasnopolsky@noaa.gov; Phone: 301-683-3742

A generic approach that allows extracting functional nonlinear dependencies and mappings between atmospheric or ocean state variables in a relatively simple form is presented. These dependencies and mappings between the 2- and 3-D fields of the prognostic and diagnostic variables are implicitly described by the highly nonlinear coupled partial differential equations of an atmospheric or ocean dynamical model. They also are implicitly contained in the numerical model output. For example, when 2-D observations like surface wind, surface currents, or sea surface elevation are assimilated in the atmospheric or oceanic data assimilation system (DAS), the impact of this information in the atmosphere state or ocean state is conveyed by the observation operator and model and observations error covariances. Several attempts have been made to extract simplified linear dependencies of such a kind from observed data [1] or model simulations [2] for the use in an ocean DAS. However, these simplified and generalized linear dependencies that are often derived from local data sets do not properly represent the complicated nonlinear relationship between the model variables. If we were able to extract/emulate these dependencies in a simple, but not overly simplified, and yet adequately nonlinear analytical form, they could be used in the DAS to facilitate a more effective 3-D assimilation of the 2-D surface data. These analytical functions and mappings could also be used for efficient model output compression, archiving, and dissemination, and for sensitivity studies and error analysis. It is only recently that steps are being taken to use the NN technique to accomplish this objective. Here we introduce a generic NN technique using a particular application to the NN emulation for sea surface height. This new and generic NN application requires a reasonable quality of the Jacobian of the NN emulation. The Jacobian analysis and an ensemble approach to improve the quality of the NN emulation and NN Jacobian are presented in [3].

Sea surface height (SSH), η, is one of the prognostic variables in ocean circulation models. The particular ocean model that was used in this study is the Real Time Ocean Forecast System (RTOFS-Global), NCEP's "ocean weather" forecasting system. Its ocean modeling component is eddy-resolving HYbrid Coordinate Ocean Model (HYCOM). This model is a primitive equation model that uses a generalized hybrid coordinate (isopycnal/terrain following (σ)/z-level) in the vertical. The hybrid coordinate extends the geographic range of applicability of traditional isopycnal coordinate (coordinates that follow the selected levels of constant water density), toward shallow coastal seas and unstratified parts of the ocean. The particular version of HYCOM used in this study covers the global domain with an average horizontal resolution of 1/12°; and 32 vertical levels, and the potential density is referenced to 20 MPa with thermobaric correction [4].

An approach based on using neural network techniques is developed here to extract the inherent nonlinear relationship between the sea surface height anomaly and the other physically related variables of an ocean model. Specifically, numerically generated grid point fields from the global HYCOM model of NCEP (National Centers for Environmental Prediction) are used for training and validating this relationship. Accurate determination of such relationships is an important first step to enhance the assimilation of the sea surface height measurements into an ocean model by propagating the signal to other dependent variables through the depth/height of the model. Since the reduced physics model has mainly a 1-D vertical structure, we assumed, in this initial attempt, that SSH, or η, at a particular model grid point (i.e., at a particular horizontal location lat/lon) depends only on the vector of state variables X at the same horizontal location. Therefore, this dependence (a target mapping) can be written as,

$$\eta = \varphi(X) \quad (1)$$

where φ is a nonlinear continuous function and X is a vector that represents a complete set of state variables, which determines SSH. In this particular case the vector X was selected as,

$$X = \{sin(\tau), \cos(\tau), \sin(lon), \cos(lon), \sin(lat), uavg, vavg, p_{bot}, temp, dp, th3d, u, v\}$$

where $\tau = 2\pi t/365$, t is the day of the year, p_{bot} is bottom pressure, dp is a profile of interfaces (vertical coordinates used in HYCOM), *temp* is a profile of temperature, *th3d* - a profile of potential density, and u and v are profiles of internal x- and y-velocities, and uavg and vavg are vertically x- and y- averaged velocities. This set of variables represents (or is used as proxy for) the physics of the deep ocean. Therefore, the mapping (1) with this particular selection of components for the vector X will not be applicable in coastal areas (depth less than ~450 m). For the coastal areas a different set of state variables should be selected. All statistics presented below in this section were calculated using the test set where coastal areas were excluded. The NN technique is applied to derive an analytical NN emulation for the relationship between model state variables, X, and SSH, or η,

$$\eta_{NN} = \varphi_{NN}(X) \quad (2)$$

using the simulated model fields which are treated as error free data. Table 1 shows statistics calculated on validation data set for SSH (simulated data), SSH_{NN} (calculated using eq. (2)), and for the difference between them.

Table 1. Validation/Interpolation Accuracy for SSH(in m). Here STD is for standard deviation of SSH, SSH_{NN}, or RMSE for their difference (last row in the table).

	Min	**Max**	**Mean**	**STD/RMSE**	**CC**
SSH	-1.848e-1	1.859e-1	3.143e-3	4.757e-2	-
SSN_{NN}	-1.021e-1	1.595e-1	1.188e-3	4.684e-2	-
SSH – SSH_{NN}	-1.517e-1	1.394e-1	-5.512e-4	5.563e-3	0.993

The Jacobian of (2) has been estimated. The derivative $\partial SSH/\partial dp$ dominates the Jacobian, it is about two orders of magnitude larger than other derivatives, constituting Jacobian. *The accuracy of Jacobian (derivatives) in terms of SSH obtained using this Jacobian is of order of several cm.* As the next step, this Jacobian will be introduced into ocean DAS to propagate SSH to the thickness of vertical layers *dp*, using equation,

$$SSH = \sum_{k=1}^{IN} \left(\frac{\partial SSH}{\partial dp}\right)_k \cdot \Delta dp_k$$

where IN is the number of vertical layers in the model.

[1] S. Guinehut, P.Y. Le Traon, G. Larnicol, S. Philipps, "Combining Argo and remote-sensing data to estimate the ocean three-dimensional temperature fields – a first approach based on simulated data", J Marine Systems, 46, pp. 85-98, 2004

[2] Mike Cooper, Keith Haines, "Altimetry assimilation with water property conservation", J Geophys. Res., 101, pp. 1059-1077, 1996

[3] V. Krasnopolsky, 2013, "The Application of Neural Networks in the Earth System Sciences. Neural Network Emulations for Complex Multidimensional Mappings", Springer, 200 pp.

[4] E.P. Chassignet, L. T. Smith, G. R. Halliwell, R. Bleck, "North Atlantic simulations with the Hybrid Coordinate Ocean Model (HYCOM): Impact of the vertical coordinate choice, reference pressure, and thermobaricity". J. Phys. Oceanogr., 33, 2504–2526.

Neural Network Technique for Gap-Filling in Satellite Observation Streams

Vladimir Krasnopolsky[1], Sudhir Nadiga[2], Eric Bayler[3], Avichal Mehra[1], David Behringer[1]
[1]NWS/NCEP/EMC, [2]IMSG at NWS/NCEP/EMC, [3]NOAA/NESDIS/STAR
Email: vladimir.krasnopolsky@noaa.gov; Phone: 301-683-3742

Operational integration/assimilation of satellite observations into operational models has three fundamental requirements/conditions: 1) gaps in the observations need to be addressed, both in the current instance and for extended gaps; 2) the data being assimilated must be for a predicted parameter; and 3) the data being assimilated must have a long data record to facilitate compilation of a robust statistical database spanning multiple seasons. Thus, integrating satellite data fields into operational models requires robust techniques to address potential gaps in the observations. In this study, we investigate one such robust gap-filling methodology — a Neural Network (NN) technique. As a test bed for this methodology we consider the use of NNs for integrating satellite ocean color fields (chl_a, Kd490, KPAR) into NOAA's operational ocean models (MOM and HYCOM). In this case NN links the ocean color variability, which is primarily driven by biological processes, with the local and remote upper ocean physical processes. We use satellite-derived surface variables — sea surface temperature (SST), sea surface height (SSH), sea surface salinity (SSS) fields, and upper layers of Argo profiles for temperature and salinity — as signatures of upper ocean dynamics in this study. This method of correlating satellite ocean color fields with other satellite observations that are currently being assimilated in the operational ocean model has the advantages of (a) being less likely to instigate assimilation errors due to dynamic imbalance, and (b) not relying on sparse *in situ* observations of ocean color.

Neural networks are very generic, accurate, and convenient mathematical models that are able to emulate complicated nonlinear input/output relationships through statistical learning algorithms [1]. Neural networks can approximate the transfer functions between a large number of possibly-interconnected inputs and multiple outputs, even when the relationships between the outputs and inputs are nonlinear and not well known. Neural networks employ adaptive weights that are tuned through training with past data sets, providing robustness with respect to random noise and fault-tolerance. Multilayer perceptrons (MLP) NNs are a generic tool for approximating such mappings. They use a family of functions like:

$$y_q = a_{q0} + \sum_{j=1}^{k} a_{qj} \cdot \phi(b_{j0} + \sum_{i=1}^{n} b_{ji} \cdot x_i); \quad q = 1, 2, \ldots, m$$

where x_i and y_q are components of the input and output vectors X and Y, respectively, a and b are fitting parameters. The activation function ϕ is usually a hyperbolic tangent, n and m are the numbers of inputs and outputs, respectively, and k is the number of neurons in the hidden layer. While NN training is a complicated and a time-consuming nonlinear optimization task, NN training needs to be done only once for a particular application. The trained NN is repeatedly applied to new data, providing accurate and fast emulations.

The satellite observations used in this study are well studied and available (or will be available soon) in near-real-time. The ocean color fields from the Visible Imaging Infrared Radiometer Suite (VIIRS) mission [2] and the SSS fields from the Aquarius mission were obtained from NASA, while the SSH and SST fields are from NOAA. The period covered in this study is 2012-2014. It is expected that the correlations between the ocean color data and current fields of SSH/SST/SSS will be dependent on location and season. Thus, lat, lon, and day of the year is included as additional inputs for NN. The NN technique is trained for the first two years

and tested on the remaining year. However, by rotating the time series, we can test for each of the three years of the data. Also, to test robustness, the input stream is varied by withholding various inputs (e.g, SSH or SSS). Finally, the root-mean-square difference (RMSD) between the observed ocean color fields and the NN output is computed and plotted and the results are analyzed.

Preliminary results of application of this methodology are shown in Figure 1. Here, daily VIIRS chl-a data (~ 20,000,000 data points) and MOM simulated fields for January 2012 through November 2013 were selected for NN training and validation. The data were split into training and validation sets by selecting every second point for training, with the other alternating points reserved for validation. NNs, with 23 inputs (satellite SSH, SST, SSS, upper levels of gridded monthly ARGO temperature and salinity, plus year, time of year (sine, cosine), longitude (sine, cosine), latitude (sine)) and one output (chlorophyll-a), but with different numbers of hidden neurons (HID = 3, 5, 10, 15, 20, 25, 30, 35, 40) were trained. The trained NN was then applied to 2014 input data for final NN validation. Figure 1 shows results for three days, December 30, 2013 (one-month projection), May 11, 2014 (six-month projection), and September 23, 2014 (9-month projection), show that the NN is able to skillfully capture the large-scale patterns of Chl-a observed in the VIIRS data, but the performance deteriorates as the projection period increases. In operational applications, this deterioration can be mitigated by using on-line adjustment of NN parameters as soon as new data become available.

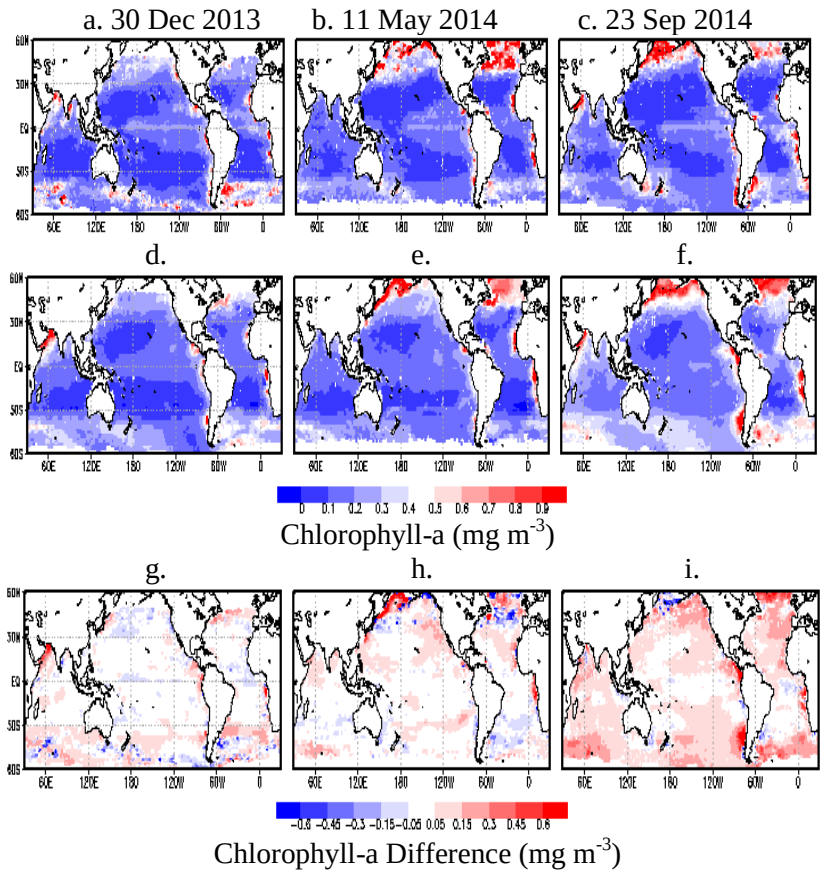

Figure 1. VIIRS chlorophyll-a (mg m^{-3}): a) 30 Dec 2013; b) 11 May 2014; and c) 23 Sep 2014; (d-f) are the same as (a-c) but are NN-predicted Chl-a; (g-i) are the difference (NN minus VIIRS).

These preliminary results demonstrate significant benefits of introducing NN approach for gap-filling in satellite observations for operational models.

[1] Krasnopolsky V., 2013, "The Application of Neural Networks in the Earth System Sciences. Neural Network Emulations for Complex Multidimensional Mappings", Springer, 200 pp.
[2] Nadiga, S., Bayler, E., Behringer, D., and Mehra, A., Towards Using Near-real-time VIIRS Ocean Color Data for NOAA's Operational Seasonal-Interannual Forecasting, 12th Annual JCSDA workshop, College Park, MD, May 21, 2014.

Upgrade of the Operational Global Real Time Ocean Forecast System

Avichal Mehra[1], Ilya Rivin[2], Zulema Garraffo[2] and Bhavani Rajan[2]

[1]Environmental Modeling Center, NCWCP, College Park, Maryland 20740, USA
[2]IMSG at Environmental Modeling Center, NCWCP, College Park, Maryland 20740, USA

1. Introduction

RTOFS (**R**eal **T**ime **O**cean **F**orecast **S**ystem)-Global is the first global eddy resolving ocean forecast system implemented operationally at NOAA/NWS/NCEP. This system is based on the 1/12 degree global HYCOM (**HY**brid **C**oordinates **O**cean **M**odel) (Bleck, 2002) and is part of a larger national backbone capability of ocean modeling at NOAA in a strong partnership with US Navy.

2. Current Status

The forecast system runs once a day and completes an eight day long forecast using the daily initialization fields produced at NAVOCEANO (**NAV**al **OCEAN**ographic **O**ffice) using NCODA (**N**avy **C**oupled **O**cean **D**ata **A**ssimilation), a 3DVAR data assimilation methodology (Cummings and Smedstad, 2013). As configured within RTOFS, HYCOM has a horizontal equatorial resolution of 0.08º or ~9 km. The HYCOM grid is on a Mercator projection from 78.64ºS to 47ºN and north of this it employs an Arctic dipole patch where the poles are shifted over land to avoid a singularity at the North Pole. This gives a mid-latitude (polar) horizontal resolution of approximately 7 km (3.5 km). After a two-day spin up with hourly NCEP's Global Data Assimilation System atmospheric fluxes, the daily forecast cycle is forced with 3-hourly momentum, radiation and precipitation fluxes from NCEP's Global Forecast System fields. Running operationally since October 2011, this global system provides boundary conditions and initializations for other operational, regional (North–West Pacific for dispersion of Fukushima radionuclides, HYCOM-HWRF hurricane coupled model) and coastal ocean forecast systems at NOS (**N**ational **O**cean **S**ervice).

3. Upgrade details and impacts

This fiscal year, the existing RTOFS-Global v1.0 will be upgraded to v1.1 in close collaboration with US Navy (Metzger et al. 2014). This upgrade developed by the Naval Research Laboratory includes the following significant modifications:

a) Number of vertical layers has been increased to 41 from 32 hybrid layers, with extra iso-level coordinate layers in the upper ~200m.
b) Ocean component HYCOM is coupled to Los Alomos National Lab's CICE (**C**ommunity **I**ce **C**od**E**) model using ESMF (**E**arth **S**ystem **M**odeling **F**ramework).
c) The bathymetry has been updated which allows grid points in shallow regions, where minimum depth is set to 5m.
d) The climatology has been updated to U.S. Navy's GDEM (**G**eneralized **D**igital **E**nvironmental **M**odel) v4.2 from v3.0.
e) An updated equation of state, 17-term sigma2 instead of a 9-term definition.

The new simulation resolves previously masked very shallow ocean regions, as an example near Bahamas (see Fig. 1). Mesoscale features in coastal regions in the Gulf of Mexico and west of the Florida Current are also better defined. The upper ocean and coastal regions are resolved with higher vertical resolution,

20 layers in the upper 150m in version 1.1 vs 11 layers in version 1.0 (Fig. 2). The Florida Current (Fig. 2, 80°W) shows a better defined baroclinicity in the new system.

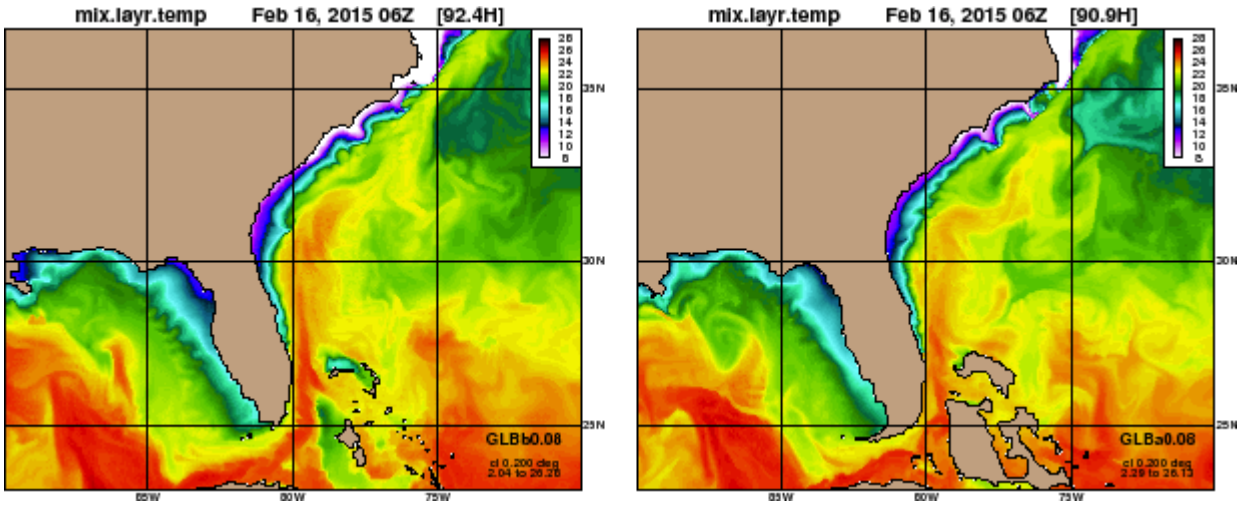

Figure 1. Sea Surface Temperature in a region covering part of the Gulf of Mexico, the Florida Current and Gulf Stream separation, for 16 February 2015 00Z, obtained by RTOFS-Global versions 1.1 (left) and version 1.0 (right). The shallow region north of Grand Bahamas is present in version 1.1 while it was masked as land in version 1.0.

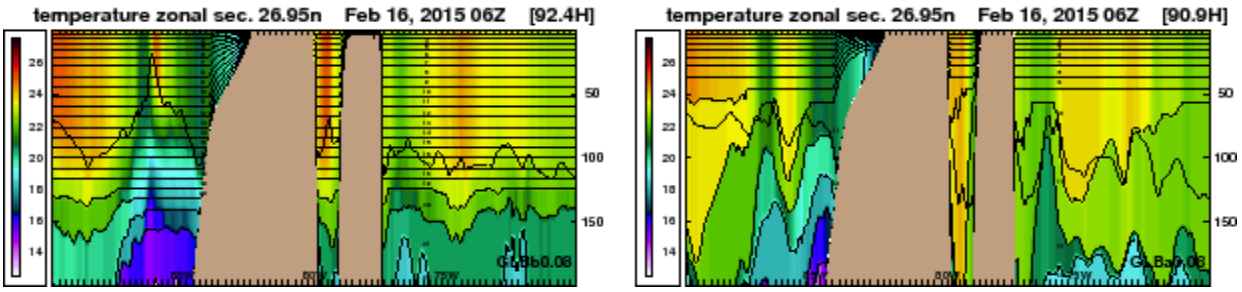

Figure 2. Section at 27N, passing just north of Grand Bahamas, from RTOFS-Global versions 1.1 (left) and version 1.0 (right). The section covers the Eastern Gulf of Mexico, Florida Current and the adjacent Atlantic Ocean, with higher vertical resolution in version 1.1.

References:

Bleck, R., 2002: An oceanic general circulation model framed in hybrid isopycnic-cartesian coordinates. *Ocean Modeling*, 4, 55-88.

Cummings, J. and O.M. Smedstad. Variational Data Assimilation for the Global Ocean. In, *Data Assimilation for Atmospheric, Oceanic & Hydrologic Applications (Vol. II)*. S. Park and L. Xu (eds). Springer, pp. 303-343, 2013.

E.J. Metzger, O.M. Smedstad, P.G. Thoppil, H.E. Hurlburt, J.A. Cummings, A.J. Wallcraft, L. Zamudio, D.S. Franklin, P.G. Posey, M.W. Phelps, P.J. Hogan, F.L. Bub, and C.J. DeHaan. 2014. US Navy Operational Global Ocean and Arctic Ice Prediction Systems. Oceanography 27(3):32–43, http://dx.doi.org/10.5670/oceanog.2014.66.

Using Near-Real-Time Satellite Ocean Color Fields (Chl-a, Kd_{490}, Kd_{PAR}) in Operational Ocean and Seasonal Forecast Systems

Sudhir Nadiga[1], Eric Bayler[2], David Behringer[3] and Avichal Mehra[3]
[1]IMSG at NOAA/NWS/NCEP/EMC, [2]NOAA/NESDIS/STAR, [3]NOAA/NWS/NCEP/EMC

Numerous modeling studies, *e.g*. Ballabrera-Poy *et al*. (2007), attest to the importance of including a solar radiation penetration-absorption scheme to better represent near-surface conditions and processes, large-scale oceanic heat transport, and coupling with the atmosphere. This team's efforts are focused on using near-real-time Visible Infrared Imaging Radiometer Suite (VIIRS) ocean color fields in NOAA's operational ocean (Mehra *et al*., 2011; Behringer, 2007) and coupled seasonal forecast systems (Saha, *et al*., 2013). To date, the work has established three key points: 1) the ocean responds vigorously to ocean color variability at all time scales, particularly in the daily-to-monthly band; 2) the composited daily VIIRS ocean color fields show significant variability; and 3) the ocean heat content response to ocean color variability can be validated with ARGO temperature and salinity profiles (Nadiga, *et al*., 2015). Employing the Modular Ocean Model version 4 (MOM4; Behringer, 2007), a preliminary study examined the differences in model response to different ocean color inputs. Three satellite chlorophyll-a (Chl-a) fields were used in this study: a) the current operational climatological monthly-mean (1997-2001) dataset from the Sea-viewing Wide Field-of-view Sensor (SeaWiFS), b) VIIRS mapped monthly-mean data (2012-2013), and c) composited VIIRS mapped daily fields (2012-2013). All fields were spatially and temporally interpolated to the model grid. The simulations were forced by daily fluxes from

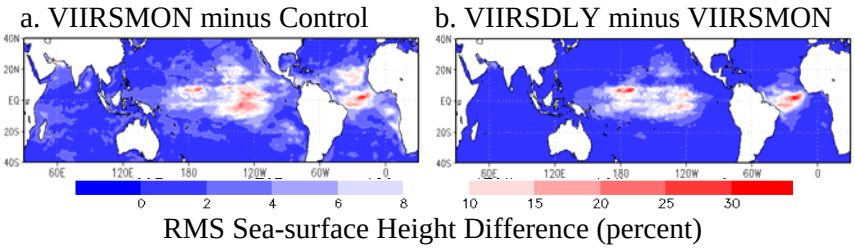

Figure 1. Root-Mean-Square (RMS) sea-surface height difference, as a percentage of RMS of Control SSH: a) VIIRSMON minus Control, and b) VIIRSDLY minus VIIRSMON.

NOAA's Climate Forecast System Reanalysis (CFSR; Saha et al., 2010). The model was weakly constrained at the surface by relaxation to daily satellite sea-surface temperature fields and a climatological mean sea-surface salinity field. Three simulations were conducted: the **CONTROL** case employed NOAA's MOM4 operational configuration, which uses the 1997-2001 climatological monthly-mean SeaWiFS chlorophyll-a fields; the **VIIRSMON** case used VIIRS monthly-mean chlorophyll-a fields; and the **VIIRSDLY** case used VIIRS daily chlorophyll-a fields. Each simulation began from the same ocean initial conditions and was run for two full years (2012-2013). Figure 1 (Nadiga *et al*., 2014) depicts that the ocean model's sea surface height (SSH) is quite responsive to differences between the prescribed Chl-a fields. While the biggest differences are seen between SeaWiFS to VIIRS (Figure 2a), due in part to representativeness issues (dominance of the 1997-1998 El Niño) with the operational SeaWiFS climatology, comparable differences are also produced from incorporating higher-frequency (daily to mesoscale) Chl-a variability (Figures 2b and 2d).

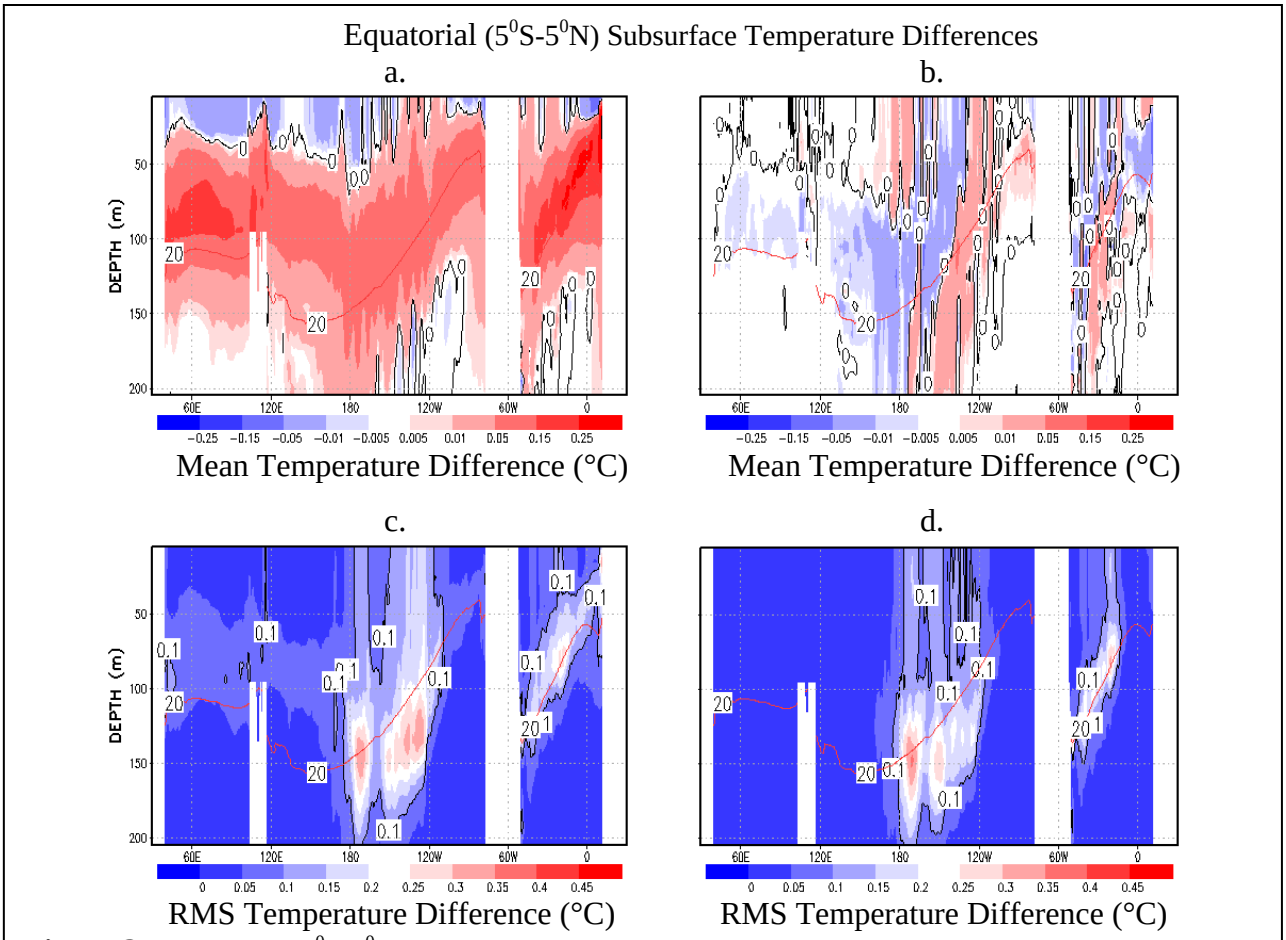

Figure 2. Equatorial (5°S-5°N) subsurface temperature differences: Mean difference **a)** VIIRSMON minus CONTROL, **b)** VIIRSDLY minus VIIRSMON; Root-Mean-Square difference **c)** VIIRSMON minus CONTROL, and **d)** VIIRSDLY minus VIIRSMON.

References:

- Ballabrera-Poy, J., R. Murtugudde, R.-H Zhang, and A. Busalacchi, 2007, Coupled Ocean-Atmosphere Response to Seasonal Modulation of Ocean Color: Impact on Interannual Climate Simulations in the Tropical Pacific, *J. Clim.*, *20*, 353-374.
- Behringer, D.W., 2007, The global ocean data assimilation system at NCEP. 11th symposium on integrating observing and assimilation systems for atmosphere, oceans, and land surface, AMS 87th annual meeting, San Antonio, TX, 12pp.
- Mehra et al. (2011) A Real Time Operational Global Ocean Forecast System. US GODAE Ocean View Workshop on Observing System Evaluation and Intercomparisons, Univ. of California Santa Cruz, CA, USA, 13-17 June 2011.(available at http://polar.ncep.noaa.gov/global/about/GODAE11_poster_d1.pdf)
- Nadiga, S., Bayler, E., Behringer, D., and Mehra, A., Towards Using Near-real-time VIIRS Ocean Color Data for NOAA's Operational Seasonal-Interannual Forecasting, 12th Annual JCSDA workshop, College Park, MD, May 21, 2014.
- Nadiga, S., Bayler, E., Behringer, D., and Mehra, A., Validation of ocean model simulations using satellite ocean color fields, AMS 95th annual meeting, (153), 2015.
- Saha, S., and co-authors, 2010. The NCEP climate forecast system reanalysis. *Bull. Amer. Meteor., Soc.*, *19*, 1015-1057.
- Saha, S., and co-authors, 2013, The NCEP climate forecast system version 2, *J. Clim.*,doi:, 10.1175/JCLI-D-12-00823.1

The Assimilation of Satellite Sea-surface Salinity Fields in Ocean Forecast Systems

Sudhir Nadiga[1], Bin Li[1], Avichal Mehra[2], Eric Bayler[3] and David Behringer[2]
[1]IMSG at NOAA/NWS/NCEP/EMC, [2]NOAA/NCEP/EMC, [3]NOAA/NESDIS/STAR

The impacts of assimilating satellite sea-surface salinity (SSS) observations into NOAA's operational modeling are examined using the Modular Ocean Model version-4 (MOM4; Behringer, 2007) for seasonal-interannual modeling and the Hybrid Coordinate Ocean Model (HYCOM; Mehra *et al.*, 2011) for near-real-time modeling. The MOM4 effort examines the use of two different SSS fields and two different levels of temporal constraint. The MOM4, forced by daily NCEP/DOE Reanalysis-2 fluxes (Kanamitsu, *et al*., 2002), employed relaxation to constrain surface temperature and salinity. Two sensitivities were tested: a) the response to the tightness of the assimilation temporal constraint and b) the response to observed SSS fields versus climatology. Four cases are compared: 1) **CTRL30** employed monthly-mean SSS climatology, the current operational configuration; 2) **AQ30** assimilated daily 1-degree resolution NASA Aquarius SSS fields (Tang *et al*., 2014), employing a 30-day relaxation period (weakly constrained); 3) **AQ10,** similar to **AQ30**, used Aquarius SSS data, but used a 10-day relaxation time period (tightly constrained); and 4) **CTRL10** also employed monthly-mean climatology, but used a 10-day relaxation period (strongly constrained). All simulations spanned the period September 2011 to August 2014 and started from the same ocean initial condition. The ocean heat content (OHC) for the top 300 m was computed for each simulation and compared with OHC computed from gridded monthly Argo float temperature and salinity profiles.

The results of comparisons show that the use of satellite SSS data creates one pattern of improvement, primarily in the tropics (Fig. 1a, 1c), while the tightening of the relaxation constraint produces a different pattern (Fig 1b). The difference **CTRL10** minus **CTRL30** is not shown, but mimics Fig 1b, although with weaker intensity. Figure 1d depicts the net affect from using near-real-time satellite SSS data. **AQ10** outperforms both the **AQ30** and the **CTRL10** in the equatorial Atlantic, equatorial western Pacific and Indian oceans by 7-10%. In other regions, the picture is mixed. There are large areas in the mid-latitudes where the AQ10 is outperformed by approximately 5-15% by the AQ30 and/or the CTRL10. Our conjecture is that the coarse-resolution operational MOM4 may not be able to resolve the significant amounts of mesoscale variability found in the daily Aquarius SSS fields. We are also investigating the correlation of restoring surface buoyancy fluxes to the large-scale spatial and temporal structure of the surface buoyancy forcing to correct systematic errors.

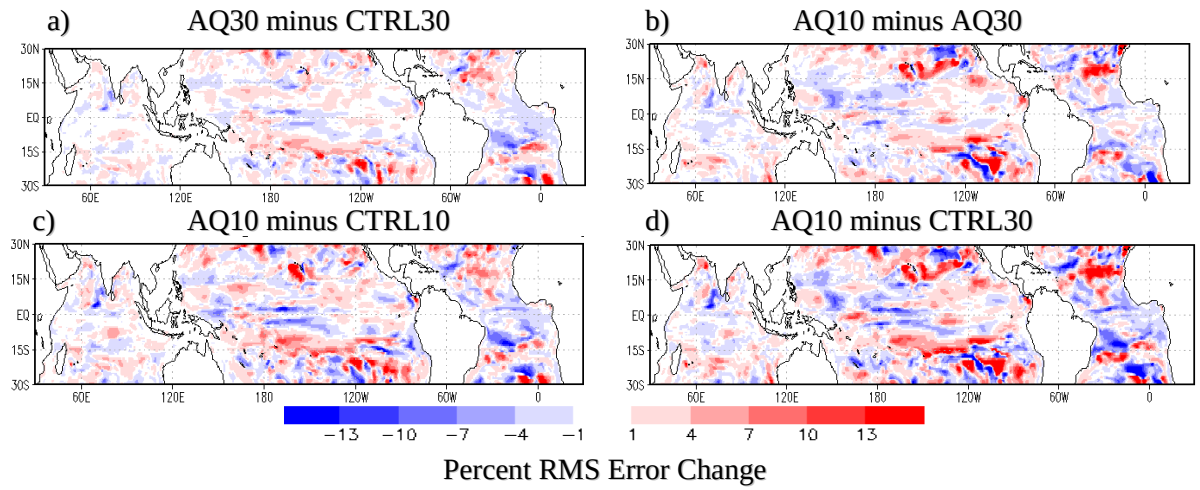

Figure 1. Change in Root-Mean-Square Error (RMSE) for ocean heat content (0-300m) for a) **AQ30-CTRL30**, b) **AQ10-AQ30**, c) **AQ10-CTRL10**, and d) **AQ10-CTRL30**; referenced to gridded ARGO monthly-mean profiles of temperature and salinity (Lebedev *et al*., 2010).

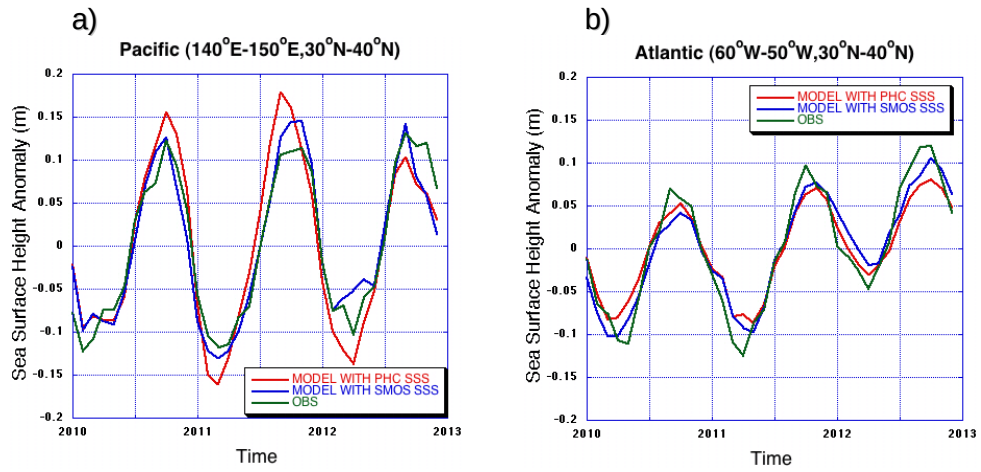

Figure 2. Comparison of mean SSH anomalies simulated by RTOFS over two sub-regions: a) North Pacific, b) North Atlantic. The satellite SSH observations are from Leuliette, *et al*., 2004.

Surface salinity in the operational near-real-time HYCOM model is relaxed to the Polar Science Center Hydrographic Climatology (PHC3; Steele *et al*., 2001). To assess the impact of near-real-time SSS data, the PHC3 climatology was replaced with monthly-mean SSS averaged from daily ESA SMOS data (Barcelona Expert Center, http://www.smos-bec.icm.csic.es/). Two sets of experiments, employing NCEP CFSR atmospheric forcings (Saha *et al*., 2010), were conducted, with the e-folding time for salinity relaxation set at 30 days × H_m/H_s, where H_m is the mixed layer depth and H_s (fixed at 15 m) is a constant reference thickness. Figure 2 shows the time evolution, 2010 through 2012, of mean sea-surface heights averaged over two selected sub-regions for both sets of experiments. The assessment validation is primarily against satellite altimetric data from NOAA/NESDIS/STAR (Leuliette *et al*., 2004). Comparisons with observations show that results with SMOS SSS data offer some improvements near the extremes of the simulated sea-surface height anomalies in the mid-latitude North Atlantic and North Pacific regions.

References:

- Behringer, D.W., 2007, The global ocean data assimilation system at NCEP. 11th symposium on integrating observing and assimilation systems for atmosphere, oceans, and land surface, AMS 87th annual meeting, San Antonio, TX, 12pp.
- Kanamitsu, M., et al., 2002, NCEP/DOE AMIP-II Reanalysis (R2), *Bull. Amer. Meteor., Soc., 83,* 1631-1643.
- Leuliette, E. W., et al., (2004), Calibration of TOPEX/Poseidon and Jason Altimeter Data to Construct a Continuous Record of Mean Sea Level Change, *Marine Geodesy*, *27*(1-2), 79-94.
- Lebedev, K. V., S. DeCarlo, P. W. Hacker, N. A. Maximenko, J. T.Potemra, and Y. Shen (2010), Argo Products at the Asia-Pacific Data-Research Center, Eos Trans. AGU, 91(26), Ocean Sci. Meet. Suppl.,Abstract IT25A-01.
- Mehra et al. (2011) A Real Time Operational Global Ocean Forecast System (RTOFS). US GODAE Ocean View Workshop on Observing System Evaluation and Intercomparisons, Univ. of California Santa Cruz, CA, USA, 13-17 June 2011.
- Saha, S., et al., 2010. The NCEP climate forecast system reanalysis. *Bull. Amer. Meteor., Soc., 19,* 1015-1057.
- Steele, M., R. , et al., (2001), PHC: A global ocean hydrography with a high-quality Arctic Ocean, *Journal of Climate*, *14*(9), 2079-2087.
- Tang, Wenqing, et al., "Validation of Aquarius sea surface salinity with in situ measurements from Argo floats and moored buoys", J. Geophys. Res. (Oceans), accepted for publication.

OCEAN DATA ASSIMILATION WITH A MODIFIED INTERMITTENT DYNAMIC RELAXATION

B.S. Strukov, Yu.D. Resnyansky, and A.A. Zelenko

Hydrometeorological Research Centre of Russian Federation (bsstr@mail.ru)

The intermittent approach to data assimilation basing on repeating prediction-analysis cycles is one of the most commonly used in meteorological and oceanographic applications. In this approach, a three-dimensional analysis is being implemented using as input the vector of all observational data $\mathbf{y}^o(t_i)$ attributable to times t_i within the analysis window $t_0 \le t_i \le t_0 + \Delta T$, where ΔT is the window width. The vector of increments $\delta\mathbf{w}^a$ obtained from this analysis is added to the first guess $\mathbf{w}^b(t_a)$ so as to obtain the analysis $\mathbf{w}^a(t_a) = \mathbf{w}^b(t_a) + \delta\mathbf{w}^a$ attributable to time t_a within the same window $t_0 \le t_a \le t_0 + \Delta T$. The analysis $\mathbf{w}^a(t_a)$ is then used as an estimate of the model initial state for calculating the first guess in the next assimilation cycle $\mathbf{w}^b(t_a + \Delta T)$.

The most serious shortcoming of such scheme is the introduction of discontinuity to the time derivatives of the state variables $\mathbf{w}$ at the time moments t_a, $t_a + \Delta T$, $t_a + 2\Delta T$, ... Abrupt change of $\mathbf{w}$ during its replacement by the analysis $\mathbf{w}^a = \mathbf{w}^b + \delta\mathbf{w}^a$ may lead to the development of unphysical disturbances due to the imbalance between different variables.

This shortcoming has been corrected in the becoming widely spread version of the intermittent scheme referred to as Incremental Analysis Updates (IAU) (Bloom et al., 1996). In IAU, the single-stage introduction of the total increment $\delta\mathbf{w}^a$ is replaced by gradual adding portions of this increment $\delta\mathbf{w}^a \Delta t / \Delta T$ during model propagation at each model time step $k = 1,2,...,K$ in a time range $t_a \le t_k \le t_a + \Delta T$:

$$\mathbf{w}_k = M_k(\mathbf{w}_{k-1}) + \delta\mathbf{w}^a \Delta t / \Delta T \,. \tag{1}$$

where Δt is the model time step, K is the number of model time steps in the assimilation window, and M_k is the forecast model operator that propagates the state from time t_{k-1} to time t_k.

The last term in (1) represents an additional forcing acting at each model time step and independent on the current model state $\mathbf{w}_k$.

Introducing the additional forcing to the model propagation operator is used in one more assimilation scheme referred to as dynamic relaxation (DR) or nudging:

$$\mathbf{w}_k = M_k(\mathbf{w}_{k-1}) - r\Delta t(\mathbf{w}_k - \mathbf{w}^a), \tag{2}$$

where r is the relaxation coefficient, and $\mathbf{w}^a = \mathbf{w}^a(t_a + \Delta T) = \mathbf{w}^b(t_a + \Delta T) + \delta\mathbf{w}^a$ is the analysis attributable to the end of assimilation window.

In contrast to (1) the additional forcing in DR depends on the current model state $\mathbf{w}_k$. Filtering properties of both schemes in their linear approximations are considered in (Bloom et al., 1996).

Both these schemes have an attractive property to suppress the undesired jumps in time of the state variables $\mathbf{w}$ during the assimilation process. Neither of these schemes, however, provides the match of the state variables $\mathbf{w}$ calculated according to (1) or (2) with the analysis $\mathbf{w}^a(t_a + \Delta T) = \mathbf{w}^b(t_a + \Delta T) + \delta\mathbf{w}^a$ at the end of the assimilation window, $t = t_a + \Delta T$. The implications of this mismatch may most clearly manifest themselves for the variables with strictly limited range of variability, such as, for example, the sea ice concentration, which by definition must be within the range (0, 1), or the sea water salinity, which must be nonnegative. Due to the nonlinearity of the model operator M_k the state variables computed by (1) may go beyond the physically permissible limits.

The mismatch can be avoided in the following modification of the intermittent scheme similar to IAU and DR:

$$\mathbf{w}_k = M_k(\mathbf{w}_{k-1}) - (\Delta T - k\Delta t)^{-1}\Delta t(\mathbf{w}_k - \mathbf{w}^a), \tag{3}$$

This scheme, which will be referred to as Modified Dynamical Relaxation (MDR), differs from the conventional relaxation (2) in that the relaxation coefficient $(\Delta T - k\Delta t)^{-1}$ is no longer constant, but increases to the end of the assimilation window ensuring the tendency $\mathbf{w} \to \mathbf{w}^a$ at $t \to t_a + \Delta T$.

A preliminary examination of scheme (3) in its comparison with scheme (1) has been performed in numerical experiments with an ocean general circulation model NEMO (Madec, 2008) coupled with a thermodynamic sea ice model LIM-2 (Fichefet et al., 1997). Used in the experiments, the ORCA1 configuration of the model had a global computational domain covered by a curvilinear tripolar grid at a base horizontal resolution of about 100 km in the main body of the domain and increasing in the near equatorial and near polar regions. The atmospheric forcing was specified using the COARE bulk algorithm with input data from the Global Forecast System (GFS) NCEP/NOAA (Environmental Modeling Center, 2003). The net heat flux at the ocean surface included the relaxation correction $\sim (\theta - \theta_s)$, where θ is the current value of water temperature in the upper model layer, and θ_s is the sea surface temperature according to GFS.

Analysis of observational data was performed with a three-dimensional variational 3DVar scheme (Tsyrulnikov et al., 2006) using as input the measurements of temperature and salinity in the upper 1500 m water layer from Argo profiling floats. The entire period of assimilation 1.01.2011-17.12.2011 included 36 cycles, each of which had a duration of 10 days.

The observational innovations being input to the 3D Var analysis were determined as deviations of observations from the first guess fields computed by the model and varied from day to day according to the FGAT methodology.

The results of these experiments are illustrated in Figure 1, which shows the vertical distributions of mean temperature and salinity deviations (biases) of measurements from the analysis averaged throughout the computational domain and through all 36 assimilation cycles. In calculating these deviations, only the independent data were used (one out of ten daily portions of data, which were excluded from the input data stream for the 3D Var analysis). Excluded from the calculation were also the measurements at a distance of less than 100 km from the nearest land.

As can be seen from Figure 1, the biases in MDR are somewhat smaller than in IAU for temperature and roughly the same for salinity. The differences of root-mean-square deviations between the two schemes were insignificant. Thus, the proposed MDR scheme has at least not worse properties in comparison with IAU. But for more substantiated conclusions, further experiments are needed over longer assimilation periods and with a more detailed tuning of the model and assimilation parameters.

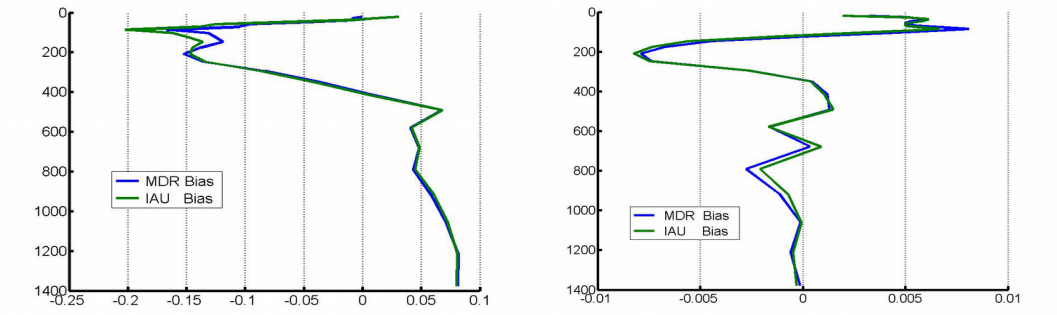

Figure 1. Vertical distributions of mean temperature (°C, left panel) and salinity (psu, right panel) deviations (biases) of independent measurements from the analysis averaged throughout the computational domain and through all 36 assimilation cycles obtained with IAU (green curves) and MDR (blue curves) schemes.

References:

Bloom, S.C., L.L. Takacs, A.M. Da Silva, and D. Ledvina, 1996: Data assimilation using incremental analysis updates. *Mon. Wea. Rev.*, **124**, 1256–1271.

Environmental Modeling Center, 2003: The GFS Atmospheric Model. *NCEP Office Note 442*. Global Climate and Weather Modeling Branch, EMC, Camp Springs, Maryland, 14 pp.

Fichefet, T., and M.A. Morales Maqueda, 1997: Sensitivity of a global sea ice model to the treatment of ice thermodynamics and dynamics. *J. Geophys. Res.*, **102**(C6), 12,609–12,646.

Madec, G., and the NEMO team, 2008: NEMO ocean engine. *Note du Pôle de modélisation*, Institut Pierre-Simon Laplace (IPSL), France, No 27, ISSN No 1288–1619.

Tsyrulnikov, M.D., P.I. Svirenko, and R.B. Zaripov, 2006: Development of a 3-D spatial ARMA-filters based analysis scheme. *Research Activities in Atmospheric and Oceanic Modelling*. WMO Rep. No. 36, 01-39–01-40.

Development of the Nearshore Wave Prediction System

Andre van der Westhuysen[1], Roberto Padilla-Hernandez[1], Pablo Santos[2], Alex Gibbs[2], Douglas Gaer[3], Troy Nicolini[4], Eve-Marie Devaliere[4], Hendrik Tolman[5]

[1]IMSG at NOAA/NCEP/EMC, College Park, MD; [2]NOAA/NWS/WFO Miami, Miami, FL; [3]NOAA/NWS/Southern Region HQ, Fort Worth, TX; [4]NOAA/NWS/WFO Eureka, Eureka, CA; [5]NOAA/NCEP/EMC, College Park, MD, UNITED STATES

andre.vanderwesthuysen@noaa.gov

1. Introduction

The demand for high-resolution forecasts of coastal processes, including waves, water levels and currents, has been steadily increasing over the past decade. The global operational multi-grid WAVEWATCH III® wave model (WW3, Tolman et al. 2002; Chawla et al. 2013), run by the National Weather Service's (NWS) National Centers for Environmental Prediction (NCEP), features a shelf-scale grid resolution of 4 arc-min (≈7.5 km), which is too coarse to resolve relevant coastal processes. It is furthermore desirable that forecasters at coastal Weather Forecast Offices (WFOs) be able to drive nearshore hydrodynamic models with their official forecast wind fields, in order to provide consistent marine forecasts to end users.

2. System description

The aim of the Nearshore Wave Prediction System (NWPS, Van der Westhuysen et al. 2013), which is integrated into NWS's Advanced Weather Interactive Processing System (AWIPS-II), is to provide high-resolution wave and surge model guidance, run in an on-demand manner by forecasters at coastal WFOs. The underlying wave model used is SWAN (Booij et al. 1999), and in future a nearshore version of WW3. The system is being deployed at all coastal WFOs in the United States (Figure 1). Output from various global or regional NOAA models are used as input to the downscaled NWPS domains, including: wave boundary conditions from the global multi-grid WW3 model (during tropical events wave boundary conditions are provided by a regional-scale simulation forced by official hurricane forecasts); water levels including tides and wind-driven surge, either from the ADCIRC-based Extra-tropical Surge and Tide Operational Forecast System (ESTOFS) or SLOSH-based probabilistic P-Surge system (tropical events); and surface current fields from the HYCOM-based Real-Time Ocean Forecast System (RTOFS). At present, the latter two fields are used as input only (one-way coupling) but in future a two-way coupling with a downscaled ADCIRC model will be included. The model computation occurs either on NCEP's production supercomputer (starting in 2015) or locally at WFOs, depending on resources. Output from the NWPS system includes: fields of integral wave parameters, fields of partitioned and tracked wave systems, and wave frequency spectra and partitioned output time series (Gerling-Hanson plots) at selected locations.

3. Results

Output from NWPS was validated using metocean observations from NDBC buoys at the shelf and nearshore. Since the NWPS domains overlap along the coast, each NDBC buoy was spatially collocated with output from the most representative model domain. Output for one cycle a day was extracted at 24 h, 48 h, 72 h and 96 h forecast windows, and compared to these observations. Figure 2 shows the resulting scatter plots and statistics for all coastal WFOs in NWS's Southern Region. The model displays satisfactory performance out to at least 72 h, with relative biases of around 5% and scatter indices of below 0.3. At later forecast hours (e.g., 96 h) the forecast guidance quality decreases, as the accuracy of the offshore wave boundary conditions and local forecaster wind fields deteriorates.

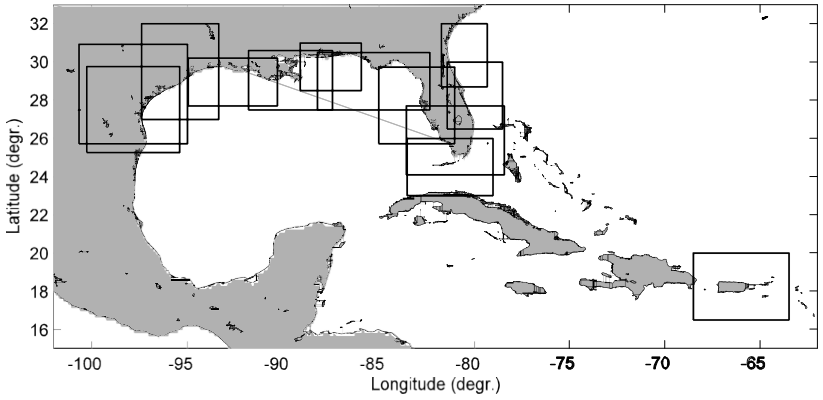

Figure 1: Example of the high-resolution NWPS wave model domains for coastal WFOs in the National Weather Service's Southern Region, including Puerto Rico and the Virgin Islands.

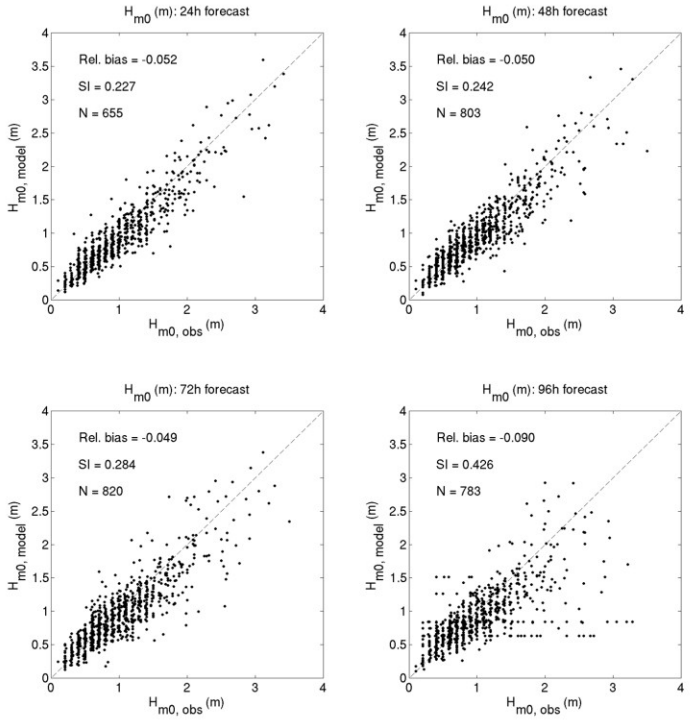

Figure 2: Forecast validation of NWPS model output at National Weather Service Southern Region WFOs during Oct 2014 to Jan 2015. Shown are model results at the 24 h, 48 h, 72 h and 96 h forecast time frames against observations at NDBC buoys.

References

Booij, N., R. C. Ris, L. H. Holthuijsen (1999), A third-generation wave model for coastal regions: 1. Model description and validation. J. Geophys. Res., 104 (C4), 7649-7666.

Chawla, A., Tolman H. L., Gerald, V., Spindler, D., Spindler, T., Alves J-H. G. M., Cao, D., Hanson J. L. and Devaliere E-M (2013), A multi grid wave forecasting model: A new paradigm in operational wave forecasting, Weather & Forecasting, Vol. 28, Issue 4, 1057-1078.

Tolman, H.L., B. Balasubramaniyan, L.D. Burroughs, D.V. Chalikov, Y.Y. Chao, H.S. Chen and V.M. Gerald (2002), Development and implementation of wind generated ocean surface wave models at NCEP. Weather and Forecasting, 17, 311-333.

Van der Westhuysen, A. J., R. Padilla-Hernandez, P. Santos, A. Gibbs, D. Gaer, T. Nicolini, S. Tjaden, E. M. Devaliere and H. L. Tolman (2013), Development and validation of the Nearshore Wave Prediction System. Presented at the 93rd AMS Annual Meeting, Am. Meteor. Soc., Austin, TX.

VERIFICATION OF THE WIND WAVE FORECASTING SYSTEM FOR THE BALTIC SEA

A.A. Zelenko, B.S. Strukov, Yu.D. Resnyansky, and S.L. Martynov

Hydrometeorological Research Centre of Russian Federation (zelenko@mecom.ru)

1. Introduction

Since 2010 the components of the system designed for operational wind wave forecasting in the World Ocean and Russian seas have been progressively putting into service in the Hydrometcentre of Russia. The forecasting is performed using as input meteorological prognostic information supplied to the spectral wind wave model WAVEWATCH III v. 3.14 (Tolman, 2009). The first results of the system's verification for the Black, Azov and Caspian Seas have been described in (Strukov et al., 2012). In this note the similar results are presented for the Baltic Sea.

2. Model configuration and input data

Bathymetry and the corresponding land-sea mask for the Baltic Sea are constructed using the GEBCO resource (The General Bathymetric Chart of the Oceans), containing the gridded bathymetry data on a global 30 arc-second grid (about 500×900 m in mid-latitudes). The wave forecasts are computed on the 4.8′×2.4′ (~4 km) geographical grid in the main body of the Baltic Sea with nested 2.4′×1.2′ (~2 km) grid in the Gulf of Finland. Atmospheric forcing needed for the model integration is taken from the prognostic meteorological data produced by the Global Forecast System (GFS) of NCEP/NOAA (Environmental Modeling Center, 2003). The wave forecasts are issued on a daily basis up to 5 days ahead starting from 00 UTC. Initial conditions for each forecast session are taken from the previous 1 day forecast. For verification purposes, the model output was written out every 15 minutes of the whole forecast period in order to minimize the time difference between predictions and satellite observations, the latter being arbitrary distributed in time and space.

3. Data for verification

Performance of the forecasting system was evaluated by comparing its product with two sources of observation data over the period from 01.04.2012 to 31.03.2013. The first of them is the satellite altimeter data on Significant Wave Height (SWH) from the Radar Altimeter Database System (RADS) supported by the Delft Institute for Earth-Oriented Space research (DEOS) (Naeije et al., 2008). The RADS is updated with altimeter data from the Earth resources satellites: Jason-2, Envisat-1, and CryoSat-2 (Figure 1).

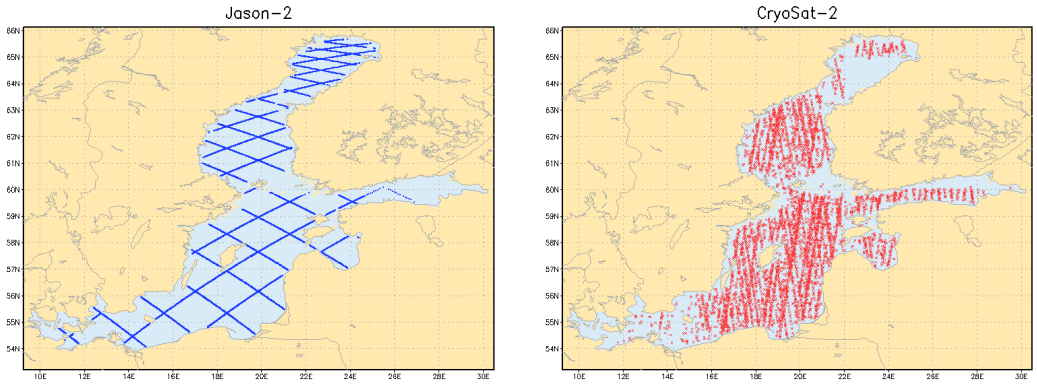

Figure 1. The network of tracks of the Jason-2 (left panel) and CryoSat-2 (right panel) satellites, the data from which were used for the forecasts verification over the Baltic Sea.

The second type of observation data used for verification are in-situ measurements of SWH from wave buoys at two locations: 59,25° N, 21° W (1.04.2012–31.03.2013) and 54,88° N, 13,87°E (1.04.2012–20.06.2012)

4. Forecast performance

Mean error (bias), root mean square error (RMSE) and correlation coefficient (CC) between forecasted and observed SWH values were used as statistical measures of the forecast performance. These statistics are presented in Table 1, and an example of scatter plots, giving an idea of the degree of compliance between forecasted and measured SWHs, are shown in Figure 2.

Table 1. Statistics of the forecast performance relative to RADS data for the verification period from 01.04.2012 to 31.03.2013.

Lead time (days)	Region	Number of observations	Bias (m)	RMSE (m)	CC
1	Baltic Sea	27156	–0.02	0.36	0.88
	Gulf of Finland	1411	–0.12	0.30	0.86
2	Baltic Sea	27156	0.04	0.42	0.85
	Gulf of Finland	1411	–0.13	0.31	0.84
3	Baltic Sea	27156	–0.04	0.51	0.77
	Gulf of Finland	1411	–0.27	0.35	0.72
4	Baltic Sea	27156	–0.07	0.62	0.60
	Gulf of Finland	1411	–0.36	0.52	0.23
5	Baltic Sea	27156	–0.14	0.59	0.57
	Gulf of Finland	1411	–0.34	0.41	0.59

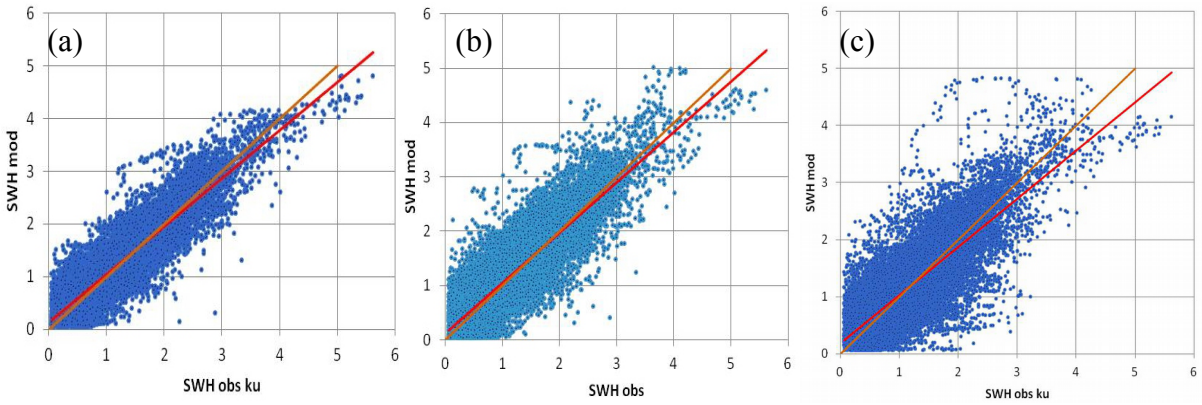

Figure 2. Scatter plots of forecasted (ordinate) and satellite measured (abscissa) SWHs for the first (a), second (b) and third (c) forecast days in the Baltic Sea. Red lines show the linear regression, yellow lines – the perfect agreement.

The absolute values of mean errors were relatively small, slightly increasing with an increase of lead time from 0.02–0.12 m to 0.14–0.34 m. In most cases the bias remained negative, indicating some underestimation of wave heights prediction in comparison with RADS estimates. The correlation coefficient varied from 0.86–0.88 for a one day lead time to 0.57–0.59 for 5 days lead time. In the comparisons with buoy measurements, the correlation coefficient was slightly higher: 0.91–0.92 for a one day lead time and 0.64–0.73 for 4 days lead time.

Deterioration of the forecast performance with increase of lead time was caused to a large extent by the increase of uncertainty of wind speed data used as input in the wave model. This is indicated by an increase of the correlation coefficient between the errors of forecasted SWH and the uncertainties of wind speed data from 0.42 for a one day lead time to 0.75 for five days lead time.

Thus, there are grounds to expect that the performance of the wind waves forecasting system will improve with improvement of weather forecasting.

References

Environmental Modeling Center, 2003: The GFS Atmospheric Model. NCEP Office Note 442. Global Climate and Weather Modeling Branch, EMC, Camp Springs, Maryland, 14 pp.

Naeije, M., R. Scharroo, E. Doornbos, and E.. Schrama, 2008: Global Altimetry Sea-level Service: GLASS. NIVR/SRON GO project: GO 52320 DEO, 107 pp.

Strukov, B.S., A.A. Zelenko, Yu.D. Resnyansky, and S.L. Martynov, 2012: Verification of the Wind Wave Forecasting System for the Black, Azov and Caspian Seas.// Research Activities in Atmospheric and Oceanic Modelling. Ed. by A. Zadra. WCRP Rpt No. 5/2012. p. 08-05–08-06.

Tolman, H.L., 2009: User manual and system documentation of WAVEWATCH III version 3.14. NOAA/NWS/NCEP/MMAB Technical Note 276, 194 pp + Appendices [Available at http://polar.ncep.noaa.gov/waves/wavewatch/].